

Article citation info:

Ma R, Zhao Y, Li J, Enhancing Distribution System Flexibility through Network Restructuring and Optimal Planning of Distributed Energy Resources, *Eksploracja i Niezawodność – Maintenance and Reliability* 2025: 27(2)
<http://doi.org/10.17531/ein/196065>

Enhancing Distribution System Flexibility through Network Restructuring and Optimal Planning of Distributed Energy Resources

Indexed by:
 Web of Science Group

Rui Ma^{a,b*}, Yuhao Zhao^{a,b}, Jianfeng Li^{a,b}

^a Electric Power Research Institute of State Grid Hebei Electric Power Co., Ltd. Shijiazhuang 050021, Hebei, China

^b State Grid Hebei Energy Technology Service Co., Ltd., Shijiazhuang 050021, Hebei, China

Highlights


- Innovative post-fault strategy with matrix rank constraints simplifies outage management.
- Optimized DER planning ensures efficient resource use and power supply during crises.
- Matrix rank-based topology boosts power system flexibility with uneven resources.

Abstract

This research introduces a novel outage management strategy (OMS) designed to enhance the resilience of distribution systems (DiSs) during severe weather-induced power outages. The approach incorporates an innovative network restructuring technique that utilizes an updated matrix to efficiently identify and reconfigure the radial network's topology following line faults. This restructuring optimizes the use of distributed energy resources (DERs) by strategically replacing connection and cross-section lines, formulated as an optimization problem solved through the social spider optimization algorithm. The key contributions include a unique matrix rank-based topology modeling method that avoids traditional empirical topological searches, proving effective in N-1, N-2, and N-3 scenarios. Comprehensive planning of DERs, encompassing both dispatchable and non-dispatchable resources, ensures optimal power supply during crises, even in systems with low to moderate DER penetration. Extensive simulations on IEEE 69-bus and IEEE 123-bus systems show that the method can sustain up to 85% of the load after line failures, significantly outperforming traditional microgrid techniques. Additionally, the strategy reduces energy resource exploitation costs by over 20% compared to conventional approaches, offering a robust solution for enhancing DiS resilience.

Keywords

distribution system flexibility, outage management strategy, network restructuring, distributed energy resources, line fault recovery.

This is an open access article under the CC BY license (<https://creativecommons.org/licenses/by/4.0/>) 

1. Introduction

1.1. Background and Aims

The growing integration of renewable energy sources (RES) and distributed energy resources (DERs) in power distribution systems presents both opportunities and challenges. As the penetration of renewable energy increases, the traditional operation and design of distribution networks, which have

been largely static and radial, must evolve to accommodate the intermittent and distributed nature of these new energy sources [1]. This evolution requires enhanced flexibility in network operations to ensure reliable and efficient power delivery, even in the face of line faults and other disturbances. Traditional distribution systems, characterized by limited

(*) Corresponding author.

E-mail addresses:

R. Ma (ORCID: 0009-0007-4066-6826) pisces_mary@126.com, Y. Zhao (ORCID: 0009-0000-9200-3839) 1792568722@qq.com, J. Li (ORCID: 0009-0002-3287-117X) lijianfeng1986@126.com,

flexibility and rigid structures, are often inadequate in addressing the complexities introduced by high levels of DER integration [2]. Recent advances in network restructuring, such as dynamic reconfiguration and the strategic placement of DERs, have shown promise in enhancing the resilience and flexibility of distribution systems. These methods enable the network to adapt to changing conditions, such as fluctuating power generation from renewables or unexpected line faults, thereby improving overall system reliability [3]. However, the existing techniques still face significant challenges, particularly in optimizing the balance between network flexibility and stability, and in minimizing the impact of faults without compromising the economic operation of the grid [4]. This study aims to develop a comprehensive framework that addresses these challenges by integrating network restructuring with advanced planning of DERs. The proposed approach focuses on enhancing the operational flexibility of distribution systems, enabling them to better handle the variability of renewable energy and the occurrence of line faults. This study seeks to identify the optimal configuration of the distribution network and the strategic deployment of DERs to improve system resilience, reduce outage durations, and maintain stable power supply under diverse fault conditions [5].

1.2. Literature Review

There is a substantial body of research dedicated to enhancing the flexibility of distribution systems through network restructuring and the strategic planning of distributed energy resources (DERs), particularly in the context of managing line faults and integrating renewable energy. Numerous studies have explored various methodologies, techniques, and frameworks to address the challenges posed by the increasing penetration of DERs in distribution networks. The following sections provide a comprehensive review of key contributions in this field, highlighting the diverse approaches and innovations proposed by various researchers.

Candas et al. [6] explored the role of network reconfiguration in enhancing the flexibility of distribution systems. Their study highlighted that traditional radial network structures limit flexibility, and dynamic reconfiguration could significantly improve system reliability

and fault tolerance. They proposed a method that leverages real-time data to reconfigure the network, reducing the impact of line faults. Shi et al. [7] focused on the integration of distributed energy resources (DERs) to enhance distribution system resilience. The authors emphasized that the strategic placement of DERs within the network could mitigate the effects of line faults by providing localized power during outages. Gantayet et al. [8] investigated the combined effect of network restructuring and DER planning on the operational flexibility of distribution systems. They introduced a multi-objective optimization framework that considers both network reconfiguration and DER deployment to minimize system losses and improve fault tolerance. Mahdavi et al. [9] presented a method for improving distribution system flexibility through adaptive network reconfiguration. The method dynamically adjusts the network topology in response to real-time fault conditions, ensuring continued power supply. Liu et al. [10] examined the impact of DERs on the flexibility and reliability of distribution systems. The study found that integrating DERs into the network, particularly renewable sources, could enhance system resilience to faults. However, the authors noted that the variability of renewable sources posed challenges, necessitating robust planning and control strategies.

Igder et al. [11] explored the role of microgrids in increasing the flexibility of distribution systems. They proposed a hybrid network structure that combines traditional grid operations with microgrids, enabling rapid isolation and recovery from faults. The study demonstrated that microgrids could significantly reduce outage times. Mahdavi et al. [12] developed a novel approach for distribution network reconfiguration that considers the stochastic nature of faults and renewable energy sources. Their probabilistic model allowed for real-time adjustments to the network structure, improving fault response. Ahrari et al. [13] investigated the role of energy storage systems (ESS) in enhancing distribution system flexibility and fault tolerance. The authors proposed an optimal ESS placement strategy that supports network reconfiguration during outages. Their findings indicated that strategically placed ESS could reduce the impact of line faults by providing temporary power, leading to a reduction in outage duration. Javadi et al. [14] proposed a comprehensive

framework for integrating DERs into distribution systems to improve flexibility and resilience. Their approach combined network reconfiguration with DER planning to create a more robust system capable of handling multiple fault scenarios. Kahouli et al. [15] analyzed the benefits of automated network reconfiguration in modern distribution systems. The authors highlighted that automation could significantly improve the speed and accuracy of network adjustments during fault conditions. Their simulations demonstrated that automated reconfiguration could reduce outage impacts. Caballero-Pena et al. [16] explored the impact of DER integration on the stability and flexibility of distribution networks. They proposed a control strategy that balances power flows between the grid and DERs during faults, ensuring stability and continuity of service. Their results indicated that the proposed strategy could reduce voltage deviations during line faults, enhancing overall system performance.

Jangdoost et al. [17] revisited the classic problem of distribution network reconfiguration to improve reliability and flexibility. They introduced an updated heuristic algorithm that rapidly identifies optimal reconfiguration strategies in response to faults. The study showed that the algorithm could reduce the time required for network reconfiguration significantly enhancing system resilience. Zakaryaseraji and Ghasemi-Marzbali [18] addressed the challenge of optimizing and securing power system operations amid rising energy demand. It introduces a technique for the strategic implementation of demand response programs (DRPs), optimal placement of distributed generation (DG), and application of DC dynamic load flow. The model optimizes DRP timing and wind unit placement, reducing congestion and significantly improving available transfer capability (ATC) rates. Ortiz-Matos et al. [19] developed a fault-tolerant control strategy for distribution systems that integrates DERs and network reconfiguration. The strategy dynamically adjusts the network topology and DER output in response to real-time fault conditions. Their study showed that this approach could reduce the number of customers affected by faults highlighting the importance of flexibility in modern distribution systems. Home-Ortiz et al. [20] investigated the potential of flexible network operation strategies in enhancing distribution system resilience. They proposed a dynamic

reconfiguration method that adapts to changing fault conditions, supported by DER integration. The study found that this approach could reduce outage durations demonstrating the value of flexibility in fault management. Aziz et al. [21] explored the use of network reconfiguration as a tool for enhancing the fault tolerance of distribution systems with high DER penetration. They proposed a strategy that optimizes reconfiguration actions based on DER availability and fault locations. Their simulations indicated that this method could reduce power loss during fault conditions, improving overall system efficiency.

Strezoski et al. [22] examined the impact of advanced distribution management systems (ADMS) on the flexibility and resilience of distribution networks. The study highlighted that ADMS could enhance fault detection and response times through better integration with DERs and network reconfiguration capabilities. Ji et al. [23] proposed a novel framework for real-time network reconfiguration in distribution systems with high levels of renewable energy. Their method used a real-time optimization algorithm that considers both the stochastic nature of renewable sources and the network's fault conditions. Nawaz et al. [24] investigated the role of demand response in enhancing the flexibility of distribution systems during line faults. The authors proposed a demand response strategy that works in conjunction with network reconfiguration to minimize the impact of faults on system operation. Schneider et al. [25] explored the potential of hybrid AC/DC microgrids in increasing the flexibility of distribution systems. They proposed a network reconfiguration strategy that leverages the advantages of both AC and DC networks to improve fault tolerance. Their study showed that hybrid microgrids could reduce the impact of line faults offering a promising solution for enhancing distribution system resilience.

Finally, Table 1 summarizes the key advantages and disadvantages of each reference, providing a clear comparison for understanding the strengths and weaknesses of various approaches in the field of distribution system flexibility and resilience

Table 1. A comparison based on the advantages and disadvantages of each reference.

Ref	Advantages	Disadvantages
[6]	Dynamic network reconfiguration enhances system reliability and fault tolerance by leveraging real-time data.	Limited flexibility in traditional radial network structures.
[7]	Strategic placement of DERs enhances resilience by providing localized power during outages.	Does not address challenges related to the variability of renewable DERs.
[8]	Multi-objective optimization minimizes system losses and improves fault tolerance by combining network restructuring and DER planning.	Complexity in balancing multiple objectives and implementation in real-world scenarios.
[9]	Adaptive network reconfiguration ensures continuous power supply by dynamically adjusting topology in real-time.	Requires sophisticated real-time monitoring and control systems.
[10]	Integration of renewable DERs enhances system resilience and fault tolerance.	Variability of renewable energy sources introduces challenges in planning and control.
[11]	Hybrid network structure with microgrids reduces outage times and enhances fault recovery.	Implementation complexity due to the need for coordination between microgrids and traditional networks.
[12]	Probabilistic model accounts for the stochastic nature of faults and renewable energy, improving fault response.	Increased computational complexity and real-time data requirements.
[13]	Optimal ESS placement reduces outage duration and enhances fault tolerance by providing temporary power.	High initial cost and maintenance requirements for energy storage systems.
[14]	Comprehensive framework combining DER integration and network reconfiguration improves system flexibility and resilience.	Potential challenges in coordinating DER operations with network reconfiguration.
[15]	Automated network reconfiguration improves speed and accuracy of adjustments during faults.	High dependency on automation technologies, which may be costly or complex to implement.
[16]	Control strategy balances power flows during faults, reducing voltage deviations and enhancing stability.	May require advanced control systems and real-time monitoring capabilities.
[17]	Heuristic algorithm rapidly identifies optimal reconfiguration strategies, enhancing system resilience.	May not always find the global optimal solution, potentially leading to suboptimal configurations.
[18]	Optimizes DRP timing and wind unit placement, reducing congestion and improving ATC rates.	May require significant adjustments in existing infrastructure to implement effectively.
[19]	Fault-tolerant control strategy reduces customer impact by dynamically adjusting network topology and DER output.	Implementation complexity due to the need for real-time adjustments and monitoring.
[20]	Dynamic reconfiguration method reduces outage durations and enhances fault management with DER support.	High reliance on real-time data and optimization algorithms, which may be computationally intensive.
[21]	Optimizes reconfiguration actions based on DER availability and fault locations, reducing power loss.	Challenges in predicting and modeling DER availability and fault impacts accurately.
[22]	ADMS enhances fault detection and response through better integration with DERs and reconfiguration capabilities.	Requires significant investment in advanced management systems and training.
[23]	Real-time optimization framework enhances fault tolerance in systems with high renewable energy penetration.	Stochastic nature of renewable energy sources adds complexity to the optimization process.
[24]	Demand response strategy minimizes fault impact in conjunction with network reconfiguration.	Effectiveness depends on customer participation and responsiveness.
[25]	Hybrid AC/DC microgrids reduce the impact of line faults, offering a promising solution for system resilience.	Integration of AC and DC systems can be complex and costly, requiring advanced control strategies.

1.3. Previous Scientific Gaps and Paper Contributions

Despite significant advancements in enhancing distribution system flexibility and resilience through network restructuring and the integration of distributed energy resources (DERs), several scientific gaps remain.

- I. Many existing methods lack effective real-time adaptability in dynamic operating conditions. While some approaches propose network reconfiguration and DER integration, they often fall short in handling sudden fault conditions or fluctuating renewable energy sources without extensive computational overhead.
- II. Previous studies frequently address network reconfiguration and DER deployment in isolation, rather than integrating them into a unified optimization framework. This fragmentation limits the ability to achieve optimal performance across both network operations and DER management simultaneously.
- III. The scalability of existing solutions is often constrained by their complexity or computational requirements. As distribution systems grow in size and complexity, methods that were effective on smaller scales may become impractical or inefficient when applied to larger networks.
- IV. Many proposed models emphasize technical performance improvements but overlook practical and economic aspects such as cost-effectiveness, ease of implementation, and the economic impact on end-users.
- V. The integration of emerging technologies, such as hybrid AC/DC microgrids and advanced distribution management systems (ADMS), is often not fully explored in the context of enhancing fault tolerance and system flexibility.

Therefore, this paper addresses these scientific gaps through several key contributions:

- I. It introduces a novel unified optimization framework that integrates network reconfiguration and DER planning into a cohesive model. This approach aims to simultaneously optimize both aspects, enhancing overall system performance and flexibility.
- II. The paper develops a real-time adaptive network reconfiguration method that dynamically adjusts to fault conditions and fluctuating energy sources. This method enhances the system's ability to maintain stability and

reliability under varying operational scenarios.

- III. A focus on scalable algorithms ensures that the proposed solutions remain effective as distribution systems expand. The paper employs efficient computational techniques to handle larger networks without compromising performance.
- IV. The proposed models include practical and economic considerations, evaluating cost-effectiveness and ease of implementation. This holistic approach ensures that the solutions are not only technically sound but also feasible for real-world application.
- V. The research explores the potential of integrating hybrid AC/DC microgrids and ADMS within the proposed framework. This integration aims to leverage the benefits of these emerging technologies to further enhance fault tolerance and system flexibility.

By addressing these gaps, the paper provides a more comprehensive approach to improving the flexibility and resilience of distribution systems, paving the way for more effective and practical solutions in the field.

2. Problem Modeling

2.1. Proposed restructuring strategy

In contemporary outage management systems (OMS) for distribution systems (DiSs), several critical challenges persist, particularly when severe weather conditions lead to widespread power outages. Existing microgrid techniques, while offering localized solutions, often fall short of addressing the following limitations:

1. **Limited Network Reconfiguration:** Traditional microgrid approaches primarily focus on local islanding, which may not be sufficient in complex, large-scale distribution networks. These techniques cannot dynamically reconfigure the entire distribution network topology in response to multiple line failures (N-1, N-2, N-3 scenarios), leading to suboptimal restoration outcomes.
2. **Inadequate Utilization of Distributed Energy Resources (DERs):** Current OMS methods often fail to fully leverage the potential of DERs during outages. This underutilization is exacerbated in scenarios with low to moderate DER penetration, where the strategic

deployment of DERs is crucial for maintaining power supply continuity. Existing approaches typically focus on either dispatchable or non-dispatchable resources, rather than an integrated approach that considers both.

3. **High Costs and Inefficiencies:** Traditional outage management techniques can be cost-intensive and inefficient, particularly when it comes to resource allocation and system recovery. Microgrid techniques often involve complex empirical topological searches, which can be computationally expensive and time-consuming, leading to delays in restoring power and higher overall costs.

The proposed OMS method directly addresses these challenges by introducing a matrix rank-based topology modeling approach that avoids empirical searches, significantly reducing computational complexity and cost. Additionally, it offers a comprehensive DER planning strategy that maximizes resource utilization, ensuring optimal power supply and resilience even in systems with varying levels of DER penetration. As shown in Figure (1), the proposed network restructuring method consists of three main steps:

- **Step 1:** The entire network is divided into several zones; each zone is defined starting from the bus post and moving downstream. If a bus, such as bus 2 in Figure (1), has several sub-bass (for example, busses 3 and 15), each sub-bass until it reaches the end bus of its feeder (for example, bus 14 and bus 22) is visited. All sub-bass

between the previous subbass and last bass, such as sub-bass 3 to 14 or sub-bass 15 to 22, are considered as a zone.

- **Step 2:** Connection switches (TS) and segmentation switches (SS) are changed to build a list of reconfiguration topologies in the event of a single-line fault in the region. Typically, there are one or two remote control zoning switches per zone. For each topology, at least one connection switch connected to the fault zone is closed. However, to avoid loops, if two connecting switches (eg, TS2 and TS4) are closed for a single-line fault, a segmentation switch (eg, SS3 or SS5) in that loop is opened. If TS2 and TS4 are closed, there are two possible topologies.
- **Step 3:** A process akin to Step 2 is undertaken to produce a list of reconfigurable topologies in the event that a two-line fault manifests in both areas. The same method can be applied to three-line faults, although the details are omitted here.

As seen in Figure (2), the fault indicator notifies the system operator of the fault and specifies the damaged region as soon as the line fault is identified. Next, the user searches the database for the topology list. Topologies that do not meet the defined constraints are discarded and the remaining options are considered for optimal distribution of energy resources planning and cost analysis.

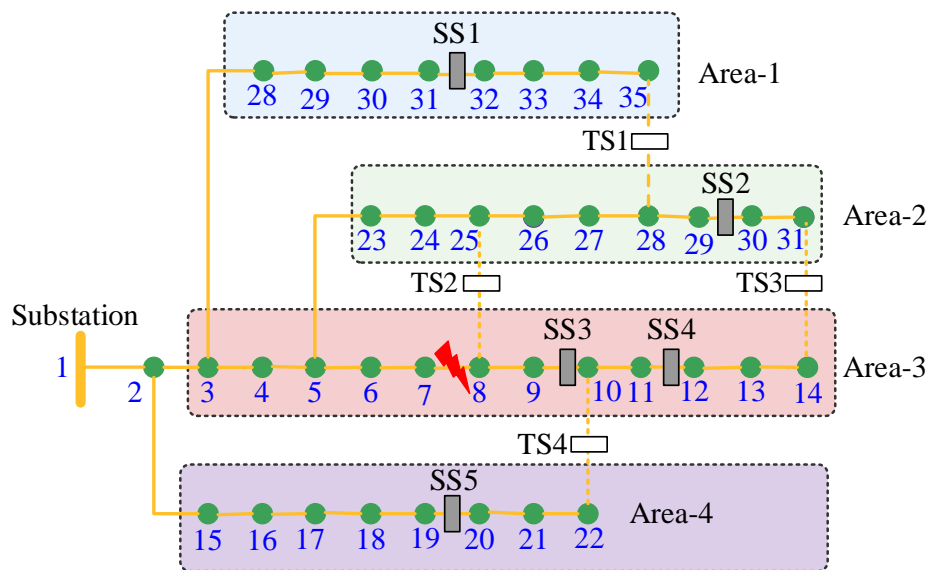


Figure 1. An example of a feeder with conventional open branches.

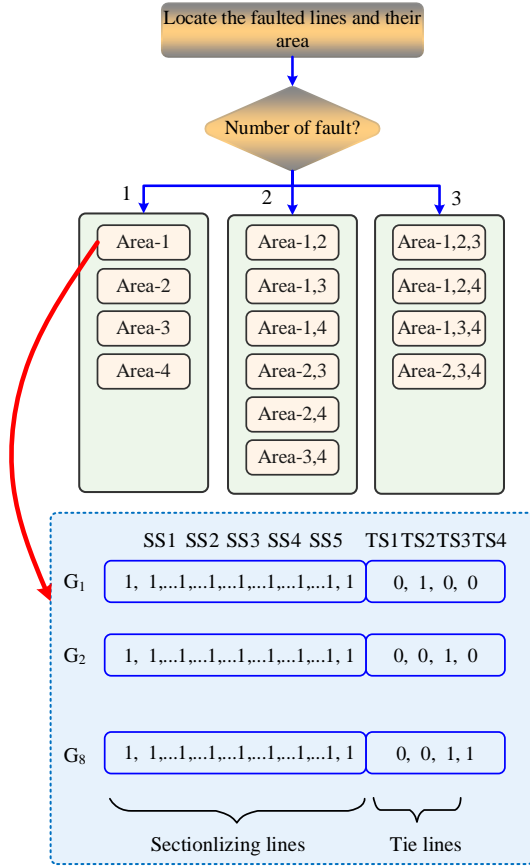


Figure 2. how the proposed restructuring strategy works

$$C(G(k)) = \text{Min} \sum_{t \in \Omega(T)} \Delta t \cdot (\sum_{i \in \Omega(L)} c_L(i) \cdot \Delta p_L(i, t) + \sum_{i \in \Omega(G)} c_G \cdot p_G(i, t)) \quad (1)$$

where c_G represents the fuel cost associated with microgrid operation.

2.3. Radial network structure limitations

In an electrical distribution network represented as a directed graph model $G(\Omega(N), \Omega(B))$, consisting of nodes ($\Omega(N)$) and branches ($\Omega(B)$). The system operator numbers each branch and node using a search technique. Under typical operating conditions, the energy flow is thought to be flowing in the positive direction in $\Omega(B)$. For the graph (G), a node-branch incidence matrix (E) is produced. The components in E , which represent the connection between nodes and branches, can have values of 0, 1, or -1. When line failures happen, the operator has to figure out the best reorganization topology to minimize load shedding and microturbine production costs while maintaining the network's radial structure. This is achieved by selectively closing the connection switches and opening the segmentation switches to connect isolated feeders with other feeders. Equations (5) through (2) specify the

2.2. The objective function

In the light of the presented analysis, as stated in equation (1), our objective function includes the critical factors in optimizing the performance of an energy management system. This function considers the total operating cost of the energy management system. In this relation, i represents the index assigned to the sub-bass, while t represents the index related to hourly time intervals. This equation integrates elements such as fuel cost associated with microgrid operation (c_G), payment of compensation for load shedding (c_L), grid output power (p_G) and the amount of load shedding (Δp_L). In addition, it considers parameters such as planning period for distributed energy sources or power outage duration ($\Omega(T)$), microgrid bus set ($\Omega(G)$), and bus set of loads ($\Omega(L)$). Equation (1) includes the two main terms of microgrid operation cost and load reduction compensation. Although cost minimization is essential, the cost component of the equation prioritizes uninterrupted power supply by taking into account the variable importance of different load types, ensuring that power remains reliably available even in adverse conditions [4]:

precise circumstances needed to preserve this radial structure. For each line, the switching state variable $s(l)$ is crucial, with values of 1 denoting closure and 0 open. This condition ensures that the protective relays appropriately open the faulty lines and that the total number of closed lines (minus the source node) equals the number of nodes. The ultimate goal is to maintain a connected graph [4]:

$$\sum_{l \in \Omega(B)} s(l) = N - 1 \quad (2)$$

$$s(l) = 0 \quad \forall l \in \Omega(B, Fau) \quad (3)$$

$$\acute{e}(l) = e(l) \cdot s(l) \quad \forall l \in \Omega(B), \acute{e}(l) \in \acute{E}, e(l) \in E \quad (4)$$

$$\text{Rank}(\acute{E}) = N - 1 \quad (5)$$

3. Estimating the probability of error

The operation management system (OMS) serves as a vital tool in reducing economic losses and energy supply disruptions caused by potential N-K incidents, especially in the face of extreme weather phenomena such as typhoons. Evaluating the likelihood of N-K occurrence is required to identify the ideal value of K which requires further research.

In practical scenarios, storm damage to overhead distribution lines occurs primarily through two mechanisms: 1) fallen tree branches striking power lines, and; 2) direct collapse due to high winds. Historical data is necessary to establish a correlation between the probability of line faults and wind speed. This paper uses a probabilistic error model that is based on the UK's NaFIRS database [26], which contains wind data values from 2003 to 2010 that recorded mean and maximum hourly wind speeds. As shown in the relation, in hurricanes, where the maximum hourly wind speed can reach 30 – 38 m/s, line error probability ($Pr(i, j)$) as a power function is modeled by the wind speed (v_w). Remarkably, this relation shows that the line fault probability is directly proportional to the line length ($l(i, j)$). For urban DiSS, $\alpha = 2 \times 10^{-17}$ and $\beta = 9.92$ is estimated. The probability of a specific scenario in the framework is calculated using equation (7) and subsequently, the cumulative probability of all scenarios with N-K possible cases is calculated using equation (8) is determined. In addition, in the case where the error probability is the same for each line, denoted as $Pr(i, j) = Pr(0)$, equations (8) to (9) become simple [4]:

$$Pr(i, j) = \alpha \cdot l(i, j) \cdot (v_w)^\beta \quad (6)$$

$$Pr(s) = \prod_{ij \in \Omega(B, Fau)} Pr(i, j) \prod_{ij \in \Omega(B) / \Omega(B, Fau)} (1 - Pr(i, j)) \quad (7)$$

$$Pr\{(N - K)Cont.\} = \sum_{|\Omega(B, Fau)|=K} \left| \prod_{ij \in \Omega(B, Fau)} Pr(i, j) \prod_{ij \in \Omega(B) / \Omega(B, Fau)} (1 - Pr(i, j)) \right| \quad (8)$$

$$Pr\{(N - k)Cont.\} = (1 - Pr(0))_{N-K} \cdot C_K(N) \cdot (Pr(0))_K \quad (9)$$

3.1. Limitations of exploitation of DERs

As indicated by Equations (27) to (10), utilization management systems are central to ensuring the efficient operation of DERs while adhering to load-spreading constraints. In this context, distributed energy sources include micro-turbines and photovoltaic systems, which are subject to limitations such as output power limitations and ramp rate limitations, which are necessary to maintain grid stability. The mentioned restrictions are shown in relations (12) - (10). In addition, load shedding constraints are applied to ensure that load shedding does not exceed predefined limits, which are controlled by demand response contracts, as stated in

Equation

$$\underline{p_G(i)} \leq p_G(i, t) \leq \overline{p_G(i)} \quad (10)$$

$$p_G(i, t) - p_G(i, t - 1) \leq \overline{UR(i)} \quad (11)$$

$$p_G(i, t - 1) - p_G(i, t) \leq \overline{DR(i)} \quad (12)$$

$$0 \leq \Delta p_L(i, t) \leq \overline{\Delta p_L(i, t)} \quad (13)$$

The system operator has the flexibility to manage thermostatic loads, optimizing their performance by adjusting settings such as water heaters and air conditioners. As stated in relation (14), constant power coefficients and conversion coefficients of reactive power variables to active power variables contribute more to network control. As shown in equation (15), in the case of photovoltaic systems, they are considered distributed non-distributable energy sources that work at their maximum power point in response to solar radiation. Limitations of AC load distribution included in equations (16) and (17) are used for accurate calculation of voltage and phase angle [27]. Also, the admittance between the sub-bass can be calculated using relations (18) and (19).

$$\Delta q_L(i, t) = \varphi(i) \cdot \Delta p_L(i, t) \quad (14)$$

$$p_{PVmp}(i, t) = \text{Min} \left(\text{Irr}(t) \cdot p_{PV, Rated}(i), p_{PV, Rated}(i) \right) \quad (15)$$

$$P(i, t) = \sum_{j=1, j \neq i}^{NB} P(i, j, t) = \sum_{j=1, j \neq i}^{NB} [B_1(i, j) \cdot (V(i, t) - V(j, t)) + B_2(i, j) \cdot (\delta(i, t) - \delta(j, t))] \quad (16)$$

$$Q(i, t) = \sum_{j=1, j \neq i}^{NB} Q(i, j, t) = \sum_{j=1, j \neq i}^{NB} [B_2(i, j) \cdot (V(i, t) - V(j, t)) - B_1(i, j) \cdot (\delta(i, t) - \delta(j, t))] \quad (17)$$

$$B_1(i, j) = \frac{r(i, j)}{(x(i, j))^2 + (r(i, j))^2} \quad (18)$$

$$B_2(i, j) = \frac{x(i, j)}{(x(i, j))^2 + (r(i, j))^2} \quad (19)$$

These limits, along with the voltage and thermal limits specified in equations (20) and (21), respectively, guarantee the reliable operation of the distribution network in different conditions. Also, in relations (22) and (23), the limits related to the active power and reactive power of buses are shown [28]. Finally, by placing relations (16) and (17) in relations (22) and (23), comprehensive relations (24) and (25) can be obtained.

$$\underline{V(i)} \leq V(i, t) \leq \overline{V(i)} \quad (20)$$

$$(P(i, j, t))^2 + (Q(i, j, t))^2 \leq (\overline{S(i, j)})^2 \quad (21)$$

$$-0.95 \times \overline{S(i, j)} \leq P(i, j, t) \leq 0.95 \times \overline{S(i, j)} \quad (22)$$

$$-0.5 \times \overline{S(i,j)} \leq Q(i,j,t) \leq 0.5 \times \overline{S(i,j)} \quad (23)$$

$$\begin{aligned} -0.95 \times \overline{S(i,j)} \leq B_1(i,j) \cdot (V(i,t) - V(j,t)) \\ + B_2(i,j) \cdot (\delta(i,t) - \delta(j,t)) \\ \leq 0.95 \times \overline{S(i,j)} \end{aligned} \quad (24)$$

$$\begin{aligned} -0.5 \times \overline{S(i,j)} \leq B_2(i,j) \cdot (V(i,t) - V(j,t)) \\ - B_1(i,j) \cdot (\delta(i,t) - \delta(j,t)) \\ \leq 0.5 \times \overline{S(i,j)} \end{aligned} \quad (25)$$

Also, as shown in relations (26) and (27), power balance is mandatory for both active power and reactive power in each system bus.

$$P(i,t) = p_{PVmp}(i,t) + p_G(i,t) - (p_L(i,t) - \Delta p_L(i,t)) \quad (26)$$

$$Q(i,t) = q_C(i,t) - (q_L(i,t) - \Delta q_L(i,t)) \quad (27)$$

3.2. Network Connectivity Constraint

Ensure that the network remains connected after reconfiguration: $\sum_{i \in \text{Active Switches}} x_i \geq N_{\text{connected}}$, where, x_i is a binary variable indicating whether switch i is active. $N_{\text{connected}}$ is the number of connections required to maintain a connected network topology.

Maintain node voltages within acceptable limits: $V_{\min} \leq V_i \leq V_{\max}$ where V_i is the voltage at node i . V_{\min} and V_{\max} are the allowable minimum and maximum voltage limits.

Additionally, during fault conditions: $|V_i - V_{\text{nominal}}| \leq \Delta V_{\max}$ where, V_{nominal} is the nominal voltage. ΔV_{\max} is the maximum permissible deviation from the nominal voltage.

Ensure that the network can effectively handle faults and maintain service: $\sum_{j \in \text{Faulted Lines}} \text{Load}_{\text{served}} \geq \text{Load}_{\text{critical}}$ where, $\text{Load}_{\text{served}}$ is the load that can be supplied during a fault. $\text{Load}_{\text{critical}}$ is the minimum load requirement for critical services.

Manage DER capacity and dispatch to meet demand: $0 \leq P_{\text{DER},i} \leq P_{\text{DER},i,\text{max}}$ and $\sum_{i \in \text{DER}} P_{\text{DER},i} \geq \text{Load Demand}$ where, $P_{\text{DER},i}$ is the power output from DER i . $P_{\text{DER},i,\text{max}}$ is the maximum capacity of DER i .

Regulate the state of charge (SOC) of storage systems to ensure operational efficiency: $\text{SOC}_{\min} \leq \text{SOC}_{\text{current}} \leq \text{SOC}_{\max}$ and $\text{SOC}_{\text{current}} = \text{SOC}_{\text{previous}} + \text{Charging} - \text{Discharging}$ where, SOC_{\min} and SOC_{\max} are the minimum and maximum SOC levels. Charging and Discharging refer to the rates of energy input and output from storage systems.

Minimize load shedding while ensuring system stability: $\text{Load}_{\text{shed}} \leq \text{Load}_{\text{max_shed}}$, Restoration Time \leq Max Restoration Time where $\text{Load}_{\text{shed}}$ is the load that is shed

during fault conditions. $\text{Load}_{\text{max_shed}}$ is the maximum allowable load to be shed. Restoration Time is the time required to restore the shed load. Max Restoration Time is the maximum allowable time for load restoration. This constraint ensures that the total load reduction due to demand response programs does not exceed the maximum allowable reduction:

$$\sum_{i \in \text{DR}} \Delta L_i \leq L_{\text{max_reduction}}$$

Where ΔL_i is the load reduction for demand response program i . $L_{\text{max_reduction}}$ is the maximum allowable load reduction from all DRPs. This constraint ensures that the demand response programs are activated within the specified time slots: $\text{DR}_{i,j} \cdot \text{Duration}_j \leq T_{\text{available},i}$

where, $\text{DR}_{i,j}$ is a binary variable indicating whether demand response program i is activated during time slot j . Duration_j is the duration of time slot j . $T_{\text{available},i}$ is the total available time for program i . This constraint ensures that the load shifted due to DRPs does not exceed the maximum allowed shift: $\sum_{i \in \text{DR}} \Delta L_{i,t} \leq L_{\text{max_shift},t}$

where, $\Delta L_{i,t}$ is the amount of load shifted for demand response program i at time t . $L_{\text{max_shift},t}$ is the maximum allowed load shift at time t .

4. Optimization Algorithm

Within the optimization community, the Social Spider Optimization (SSO) Algorithm provides a compelling method for solving complex optimization problems. In the SSO, the optimization search space is conceptualized as a multidimensional, intricate spider web. Each point within this web represents a potential solution to the optimization problem, with each solution occupying a distinct position. This web not only holds these solutions but also serves as a medium for the transmission of vibrations generated by the spiders [29].

The spiders themselves are the primary agents driving the optimization process in the SSO. At the start of the algorithm, a fixed number of spiders are strategically positioned across the web. Each spider, denoted by the letter s , maintains a memory that stores several critical pieces of information: its current position in the web, the fitness score of that position, the deviation of its target from the previous iteration, and the number of iterations since it last modified its target vibration. This memory also records the exact movements made in the

previous iteration and utilizes a mask to guide its subsequent movements. The first two pieces of information define the individual status of each spider, while the remaining data help guide the spiders to new positions.

It is noteworthy that spiders have highly accurate vibration-sensing capabilities. They can not only detect different vibrations passing through a web but also measure their intensity. In the SSO, when a spider moves to a new position that differs from its previous one, it generates vibrations. The suitability of the new position is closely correlated with the intensity of these vibrations. As the vibrations propagate through the web, other spiders can detect them, facilitating the sharing of individual spider information across the network. This interaction results in the creation of a collective reservoir of social knowledge.

The concept of vibration is crucial in the SSO and sets it apart from other meta-heuristic algorithms. In SSO, vibrations are characterized by two main features: the source location and the intensity. The source location corresponds to the search space of the optimization problem, with the spider vibrating at its position as it moves. $P_a(t)$ represents the location of the spider at time t . The symbol $I(P_a(t), P_b(t))$ denotes the intensity of vibration detected by a spider at location $P_b(t)$ at time t , with the vibration source located at $P_a(t)$. The intensity of vibration at the source point, $F(P_s(t))$, is proportional to the spider's position. Equation (28) establishes this intensity value, where C is a small constant that ensures all fitness values remain above C , providing a measure of reliability. It is important to note that this discussion focuses primarily on minimizing issues within this context. Formula (28) considers several key points [29]:

1. All vibration intensities related to the optimization problem are inherently positive.
2. Positions with higher fitness values correspond to stronger vibration intensities.
3. Vibration intensity does not increase excessively as a solution approaches the global optimum, which helps prevent disruption of the vibration attenuation process.

$$I(P_a(t), P_b(t)) = \log \left(1 + \frac{1}{F(P_s(t)) - C} \right) \quad (28)$$

As vibrations propagate through the web, they naturally

lose energy over distance, a phenomenon incorporated into the SSO design. The separation between two spiders denoted as $D(P_a(t), P_b(t))$, is calculated using Equation (29). The reduction of vibration intensity over distance is determined using Equation (30). In this context, r_a is a user-adjustable parameter within the range $(0, \infty)$ that controls the rate of attenuation. A larger value of r_a reduces the effect of vibration damping as it travels through the web [29]:

$$D(P_a(t), P_b(t)) = \|P_a(t) - P_b(t)\|_1 \quad (29)$$

$$I(P_a(t), P_b(t)) = I(P_a(t), P_a(t)) \cdot e^{-\left(\frac{D(P_a(t), P_b(t))}{\sigma \cdot r_a}\right)} \quad (30)$$

In the next step, the algorithm defines the goal function and its solution space, forming the optimization process's foundation. Following this, the method creates an initial population of artificial spiders for optimization, based on the specified parameters. Throughout the SSO simulation, this population remains constant, with each spider's vital data stored in a fixed-size memory.

The spiders are randomly positioned across the search space, and their fitness values are calculated and recorded. Initially, each spider's goal vibration is set to its current location, with a vibration strength of zero. All additional attributes for each spider are similarly initialized to zero. This concludes the first phase of the algorithm and marks the beginning of the iteration phase, where the artificial spiders are utilized to perform the search.

During the iteration phase, the algorithm performs multiple iterations. In each iteration, every spider moves to a new location and evaluates its fitness level. The iteration process can be divided into discrete sub-steps, including vibration generation, random motion, mask modification, fitness evaluation, and constraint management.

Before updating the overall optimal value, the algorithm calculates the fitness levels for each artificial spider at each position within the web. Fitness values are evaluated once per iteration for each spider. Using Equation (28), spiders generate vibrations at their respective locations. Once all vibrations are generated, the algorithm simulates their propagation, as described in Equation (30). In this process, each spider detects vibrations from all other spiders, denoted by the symbol v . These vibrations provide information about the source location and the attenuated intensity of the vibrations.

After receiving v , each spider identifies the strongest vibration, denoted as $v_s^{Best}(t)$, from V , which is the vector representing the set of v . The spider compares this intensity with its target vibration intensity $v_s^{Tar}(t)$ stored in its memory. If $v_s^{Best}(t)$ is stronger, the spider updates $v_s^{Tar}(t)$ to match $v_s^{Best}(t)$ and resets $c_s(t)$, which tracks the number of iterations since the spider last changed its target vibration. If $v_s^{Best}(t)$ does not exceed the intensity of the current $v_s^{Tar}(t)$, the original $v_s^{Tar}(t)$ is retained, and c_s is incremented by one. The source positions V and $v_s^{Tar}(t)$ are represented as $P_{s,i}$ and $P_s^{Tar}(t)$, respectively.

Next, the algorithm uses a mask to guide each spider's movement through a random walk towards $v_s^{Tar}(t)$. Each spider contains a binary m -dimensional mask of length D , where D represents the size of the optimization problem. Initially, all values in the mask are set to zero. Spider s has a probability of altering its mask in each iteration, calculated as $1 - p_c^{cs}(t)$. If the mask is to be modified, each bit in the vector has a probability p_m of being set to one, and a probability $1 - p_m$ of remaining zero. The parameter p_m is user-controlled and falls within the range $(0,1)$. Each bit in the mask is changed independently, without reference to its previous state. If all bits are zero, a random bit is set to one.

Once the mask is determined, a new position $P_{s,i}^{Fo}(t)$ for each spider is calculated based on the mask. The value of each dimension $P_{s,i}^{Fo}(t)$ is determined using Equation (31), which incorporates random integers and the corresponding values from the spider's dimension mask.

$$P_{s,i}^{Fo}(t) = \begin{cases} P_{s,i}^{Tar}(t) & \text{if } m_{s,i}(t) = 0 \\ P_{s,i}^r(t) & \text{if } m_{s,i}(t) = 1 \end{cases} \quad (31)$$

$$P_s(t+1) = P_s(t) + r \cdot (P_s(t) - P_s(t-1)) + (P_s^{Fo}(t) - P_s(t)) \odot R \quad (32)$$

$$P_{s,i}(t+1) = \begin{cases} r \cdot (x_i^{Up} - P_{s,i}(t)) & \text{if } P_{s,i}(t+1) > x_i^{Up} \\ r \cdot (P_{s,i}(t) - x_i^{Down}) & \text{if } P_{s,i}(t+1) < x_i^{Down} \end{cases} \quad (33)$$

The OMS aims to enhance the flexibility, reliability, and efficiency of distribution systems through optimized network reconfiguration, distributed energy resource (DER) integration, and dynamic load management. Here is a discussion of how each step of the SSO algorithm contributes to achieving these objectives:

4.1. Initialization and Parameter Setting

- **Flexibility Enhancement:** During initialization, the SSO algorithm sets up the initial swarm parameters and defines the problem space, including network configuration and DER placement. This step ensures that the algorithm starts with a diverse range of solutions, which is crucial for exploring different configurations and optimizing flexibility.
- **Efficiency:** Proper parameter setting helps in defining the search space more effectively, leading to quicker convergence and reducing computational resources required for optimization.

4.2. Swarm Position Update

- **Reliability Improvement:** The position update phase involves adjusting the positions of the particles (potential solutions) based on their own experiences and those of their neighbors. This step allows the algorithm to explore different network configurations and DER placements, which can enhance the reliability of the system by identifying configurations that improve fault tolerance.
- **Dynamic Load Management:** By updating positions iteratively, the algorithm can better model and adapt to changing load conditions and fault scenarios, contributing to improved dynamic load management.

4.3. Evaluation and Fitness Calculation

- **Flexibility and Efficiency:** In this phase, the algorithm evaluates the fitness of each solution based on defined criteria such as system flexibility, fault tolerance, and operational efficiency. This step ensures that only the most promising configurations are retained, aligning the algorithm's objectives with the OMS goals of enhancing system flexibility and efficiency.
- **Reliability:** Fitness calculation incorporates the impact of network reconfiguration and DER integration on system reliability, ensuring that solutions that improve fault response and system robustness are prioritized.

4.4. Selection and Replacement

- **Optimization of System Performance:** The selection and replacement step involves choosing the best-performing solutions from the swarm and discarding less effective ones. This process aligns with the OMS objectives by focusing on configurations that provide optimal performance in terms of flexibility, reliability, and efficiency.
- **Cost-Effectiveness:** By selecting solutions that meet performance criteria while being computationally feasible, this step ensures that the proposed configurations are not only effective but also practical and cost-effective for real-world implementation.

4.5. Convergence Check and Iteration

- **Continuous Improvement:** The convergence check assesses whether the algorithm has reached an optimal or satisfactory solution. Iterating through this process allows the algorithm to continuously refine solutions, ensuring that the final network configuration and DER placements meet the OMS objectives of enhanced flexibility, reliability, and operational efficiency.
- **Adaptability:** Iterative refinement helps the algorithm adapt to new information and changing conditions, ensuring that the solutions remain

relevant and effective as system parameters evolve.

By aligning each step of the SSO algorithm with the OMS objectives, the methodology effectively supports the goals of enhancing distribution system performance, addressing both current and future operational challenges. This alignment ensures that the solutions derived from the algorithm contribute to improved system flexibility, reliability, and efficiency in a practical and scalable manner.

5. Numerical results

During severe weather events such as hurricanes, outages of distribution lines can occur unpredictably. In order to examine our approach's performance in depth, this part deals with extensive case studies that include IEEE 69-bus and IEEE 123-bus systems [30]. The IEEE 69-bus and IEEE 123-bus systems are chosen for their recognized status as benchmark models in power system research, enabling effective validation of optimization techniques. The 69-bus system represents

a moderately complex distribution network, suitable for fundamental optimization problems, while the 123-bus system offers a more detailed and complex scenario for comprehensive evaluation. Both systems simulate realistic distribution conditions, balancing complexity and computational feasibility, making them ideal platforms for validating methodologies in practical distribution system scenarios.

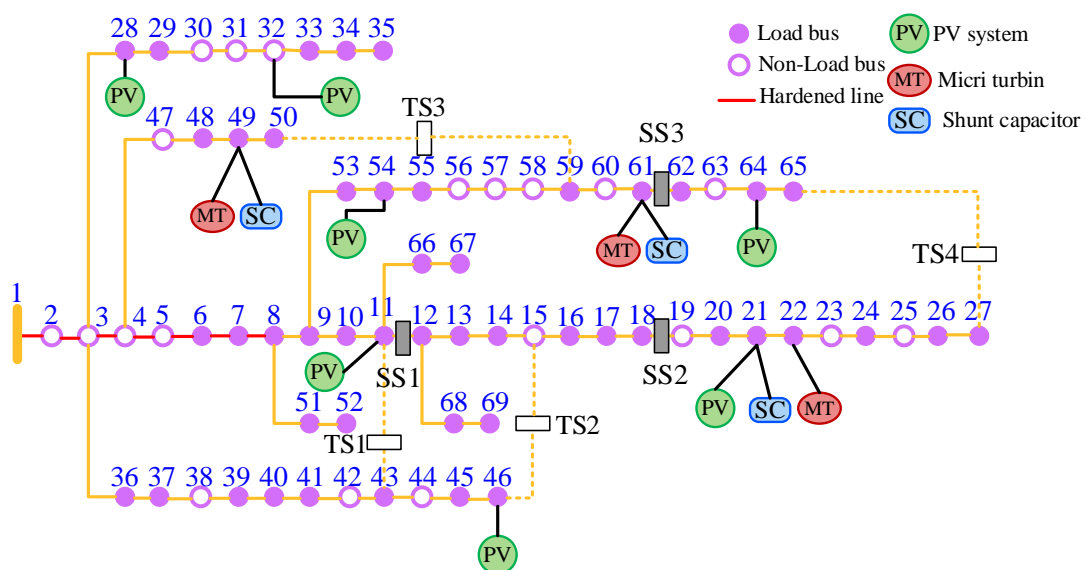
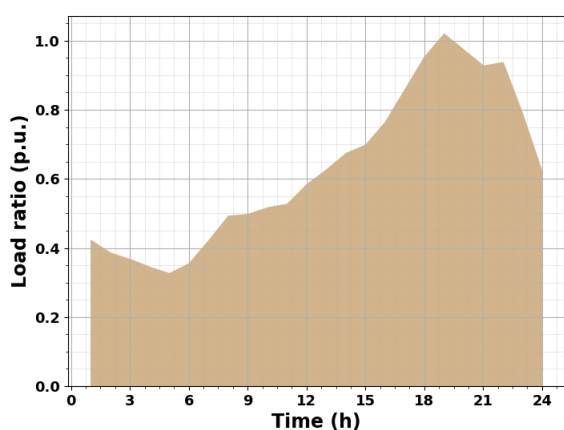


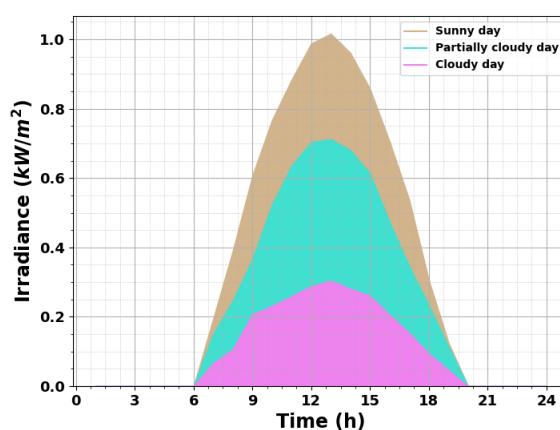
Figure 3. Considered IEEE 69 bus power system.

As seen in Figure (3). Micro-turbines, shunt capacitors, and solar systems are added to the upgraded IEEE 69-bus system. This network has four tie switches and three axial shunt switches. To accurately test the resilience of the OMS, we have amplified the load for each node. The IEEE 69 bus core system increases the potential for voltage violations by a factor of 2.0. Additionally, we set V_{Min} to 0.94 p.u. We have adjusted, and we have prioritized overload recovery over maintaining the exact voltage range when unexpected events occur. The optimization works in one-hour intervals with

a load base amount of 1 MVA and a voltage base of 12.470 kV. Figure (4) shows the desired load of the system as well as the amount of solar radiation for one day of operation. We also consider the worst-case scenario, i.e. a cloudy day where the solar radiation is reduced to only 30% of the sunny day level. During normal operating hours, i.e. 01:00 - 12:00, all power injections are equal to zero. After that, power flow calculations are performed according to the relationships presented in the modeling.



(a) Load



(b) Solar irradiation

Figure 4. Load profile and solar radiation in the desired system.

5.1. Error on two lines

- 1) Scenario 1: Lines 10-11 and 54-55 are interrupted at 13:00.
- 2) Scenario 2: Lines 12-13 and 47-48 are interrupted at 13:00.

Topologies obtained in scenarios 1 and 2 are shown in Table (2). Scenario 1 requires a total computation time of 0.532 s and provides ten candidate topologies. In contrast, scenario 2 requires 0.351 s and provides nine candidate topologies. The minimum cost for scenarios 1 and 2 is \$4352 and \$5912, respectively. It is noteworthy that certain topologies (such as G2 and G4 in scenario 1) have been excluded due to the inability of the algorithm to identify a practical solution for scheduling distributed generation resources. In a similar way, some topologies (eg, G4 in scenario 2) are eliminated due to rank constraints. Figure (5) graphically shows the optimal topologies for both scenarios, while the micro-turbine planning curves and load reduction related to the optimal topologies are shown in Figure (6) and

Figure (7) respectively. It can be seen that the load reduction is almost the same for both scenarios, however, scenario 2 shows much higher costs due to the deactivation of more critical loads at 19:00 as the time relationship of maximum load reduction for both scenarios. To gain further insight, we examine bus voltages at each time interval. It is apparent that during peak hours, some buses in scenario 2 struggle with low voltages. This voltage drop is attributed to significant impedances along lines 57-58, 60-61, and 63-64, which are exacerbated by the heavy current flowing through these lines. Importantly, this low voltage problem also appears during normal operation when the load level peaks. However, during blackout periods, the primary duty is to serve a higher load, which increases the importance of maintaining accurate voltage parameters. Consequently, in order to accept larger loads, the voltage limit might be decreased. To enhance voltage profiles, operators could think about placing shunt capacitors next to heavy-load buses. All things considered, the bus voltage limit can be freely lowered during the reorganization phase, possibly removing load shedding

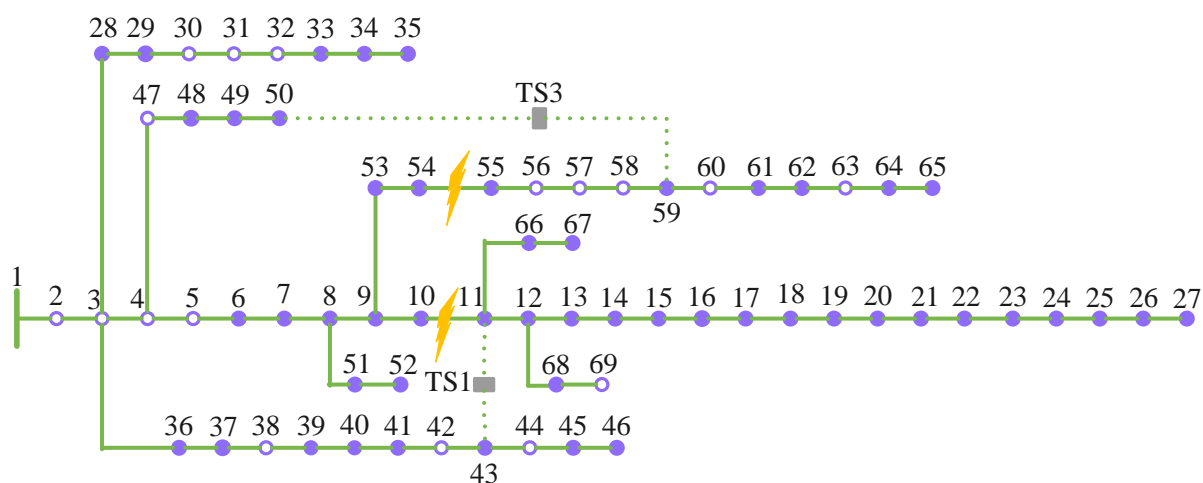
brought on by voltage breaches.

Table 2. Topologies of the system obtained in the event of 2 errors

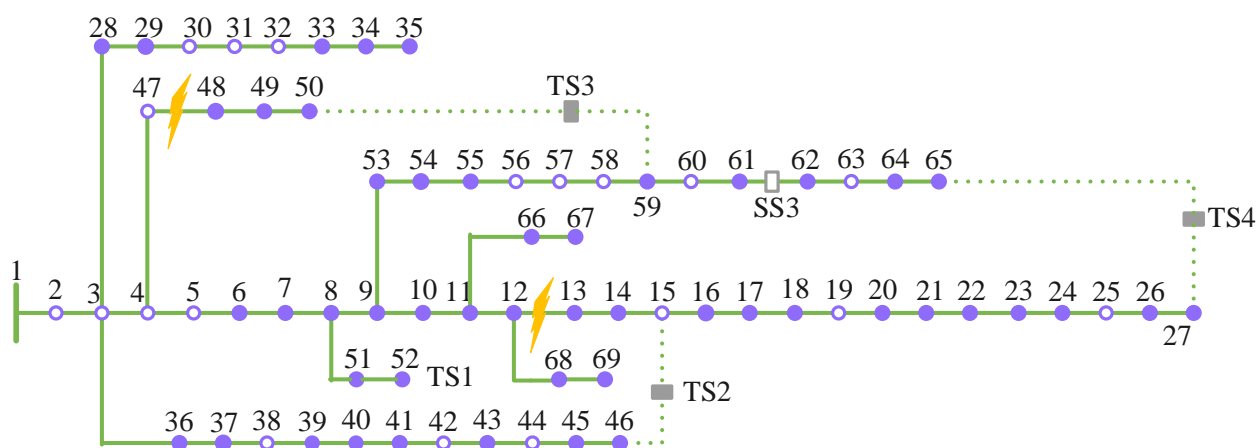
Topologies	Scenario 1		Scenario 2	
	Switching action	Operation cost (\$)	Switching action	Operation cost (\$)
G1	Close: TS1, TS3	4352	Close: TS1, TS3	NC
G2	Close: TS1, TS4	NF	Close: TS2, TS3	6248
G3	Close: TS2, TS3	4352	Close: TS3, TS4	8395
G4	Close: TS2, TS4	NF	Close: TS1, TS3, TS4 – Open: SS1	NC
G5	Close: TS3, TS4	NF	Close: TS1, TS3, TS4 – Open: SS2	NC
G6	Close: TS1, TS3, TS5 – Open: SS1	NF	Close: TS1, TS3, TS4 – Open: SS3	NC
G7	Close: TS1, TS3, TS5 – Open: SS2	4413	Close: TS2, TS3, TS4 – Open: SS2	6801
G8	Close: TS1, TS3, TS5 – Open: SS3	6524	Close: TS2, TS3, TS4 – Open: SS3	5912
G9	Close: TS2, TS3, TS4 – Open: SS2	4407	Close: TS1, TS2, TS3 – Open: SS1	NC
G10	Close: TS2, TS3, TS4 – Open: SS3	6442		

NF: Topology is radial, but there is no feasible solution

NC: Rank(E)<68 and topology is not a connected graph



a) Scenario 1



(b) Scenario 2

Figure 5. optimal topology of the system obtained in different scenarios in N-2 mode.

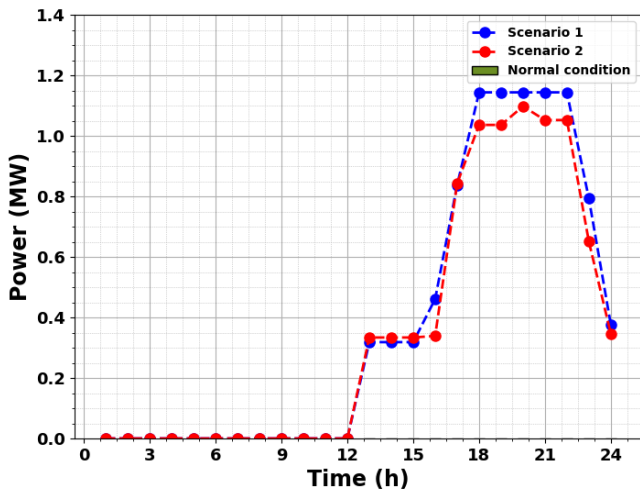


Figure (6) Optimal planning of micro turbine in different scenarios in N-2 mode

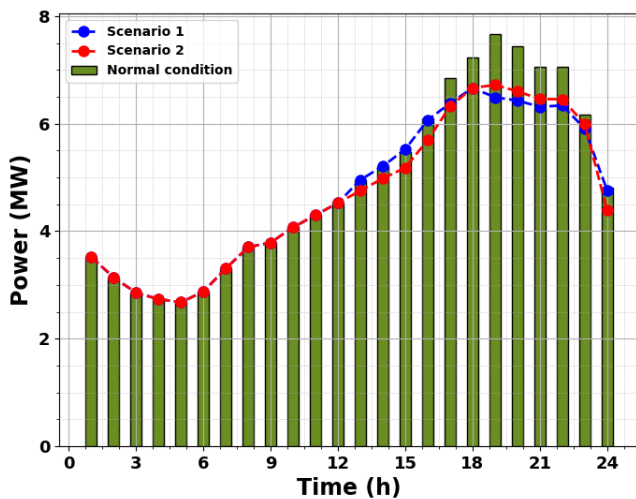


Figure 7. load changes in different scenarios in N-2 mode.

5.2. Error on three lines

In this section, we focus on the analysis of two precautionary N-3 scenarios:

- 1) Scenario 3: At 13:00, we consider a simultaneous line outage on lines 12-13, 38-39 and 4-47.
- 2) Scenario 4: At 13:00, we consider simultaneous line outages in lines 36-37, 47-48 and 62-63.

Table (3) provides a comparative analysis of the topologies obtained for scenarios involving three simultaneous line faults in the IEEE 123-bus system. The data illustrate the trade-offs between operational costs and network reconfiguration strategies under different fault conditions. In Scenario 4, the topologies with operational costs ranging from \$5,825 to \$6,129 show that closing switches TS1, TS2, and TS4 provide the most cost-effective solutions. Topologies such as G1 and

G2, which involve these switches, effectively manage the faults while keeping costs relatively low. The minimal operational costs in Scenario 4 suggest that these configurations offer a balanced approach to fault management, maintaining network reliability without excessive expenditure. In contrast, in Scenario 3, operational costs are notably higher, ranging from \$7,329 to \$8,327. The increased costs in Scenario 3, despite similar switching actions, indicate that the fault conditions create more complex challenges, leading to more expensive reconfiguration requirements. Several topologies in both scenarios are marked as "NC" (No Connected), highlighting the infeasibility of these configurations in maintaining a connected network under fault conditions. This underscores the practical limitations of certain topologies, emphasizing the importance of selecting feasible configurations that ensure continuous network connectivity. The presence of infeasible topologies reveals that not all theoretically optimal solutions are practical in real-world scenarios, reinforcing the need for robust fault management strategies that maintain system stability. The consistent use of switches TS1, TS2, and TS4 in the lower-cost topologies suggests their critical role in achieving an optimal balance between cost and network reliability. These switches are effective in minimizing operational costs while addressing fault conditions. On the other hand, topologies with additional switch openings, such as G4, lead to higher operational costs. This indicates that while these configurations might offer better fault tolerance, they come at a greater expense. The higher costs associated with more complex switching actions reflect the additional operational burden and the increased need for robust fault management. In summary, the results highlight that while some topologies provide cost-effective solutions, others, although potentially offering better fault management, incur higher operational costs. The balance between cost and network reliability is crucial in selecting the optimal topology for managing multiple simultaneous faults, emphasizing the need for careful consideration of both economic and practical aspects of network reconfiguration.

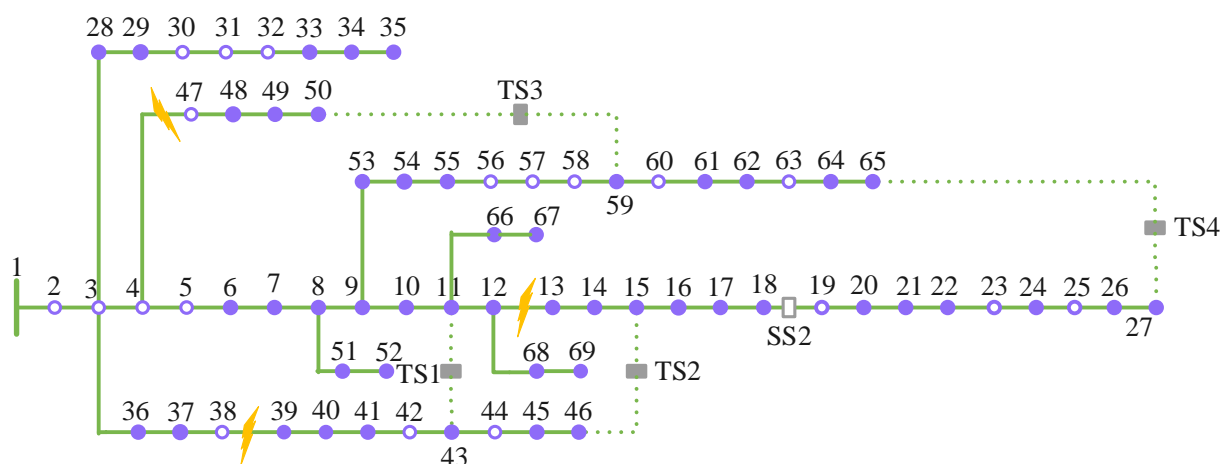
In Figure (8), the optimal topologies for both scenarios can be seen, which are presented with the microturbine planning curves and load reduction according to the optimal topologies

shown in Figure (9) and Figure (10), respectively. A careful observation shows that the maximum load shedding for both scenarios is realized at 19:00. As can be seen from these figures, in case of an error at 1:00 p.m., the micro turbine increases its production at 1:00 p.m. - 11:00 p.m. in

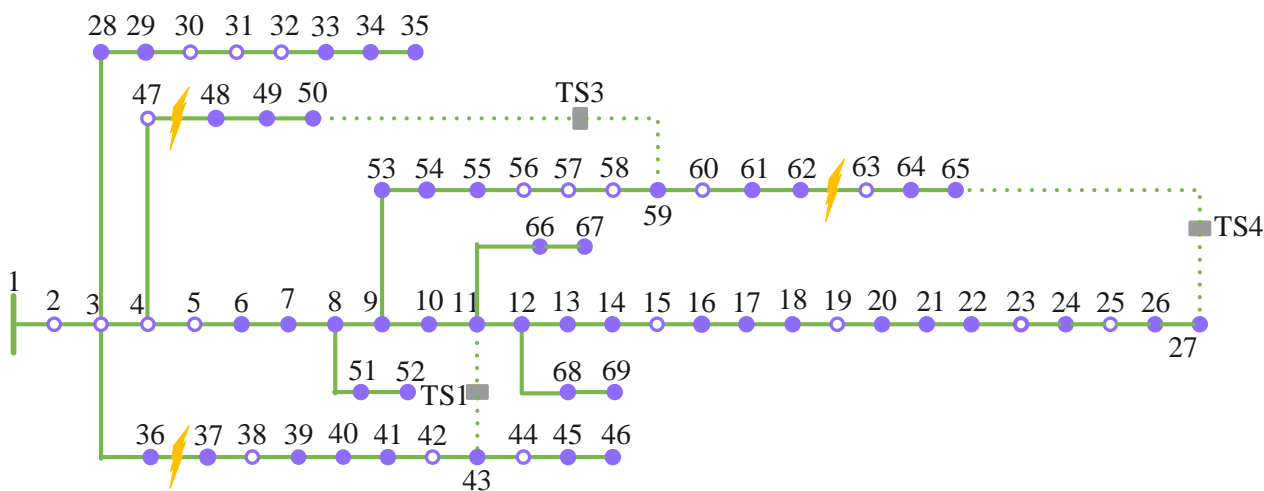
both scenarios, which is more in scenario 3. The eye comes. But after reaching the maximum production of microturbines at 17:00 and not being able to supply the system loads, the load reduction during these hours of operation is much more than other hours after the error.

Table 3. Topologies of the system obtained in case of 3 errors.

Topologies	Scenario 3		Scenario 4	
	Switching action	Operation cost (\$)	Switching action	Operation cost (\$)
G1	Close: TS1, TS2, TS4	8327	Close: TS1, TS2, TS4	5825
G2	Close: TS2, TS3, TS4	9413	Close: TS2, TS3, TS4	5843
G3	Close: TS1, TS2, TS3, TS4 – Open: SS1	NC	Close: TS1, TS2, TS3, TS4 – Open: SS1	6129
G4	Close: TS1, TS2, TS3, TS4 – Open: SS2	7329	Close: TS1, TS2, TS3, TS4 – Open: SS2	NC
G5			Close: TS1, TS2, TS3, TS4 – Open: SS3	NC



(a) Scenario 3



(b) Scenario 4

Figure 8. obtained the optimal topology of the system in different scenarios in N-3 mode.

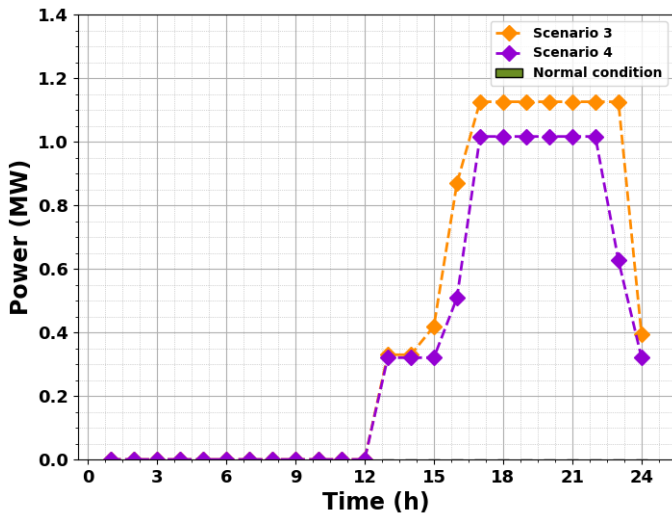


Figure 9. optimal micro turbine planning in different scenarios in N-3 mode.

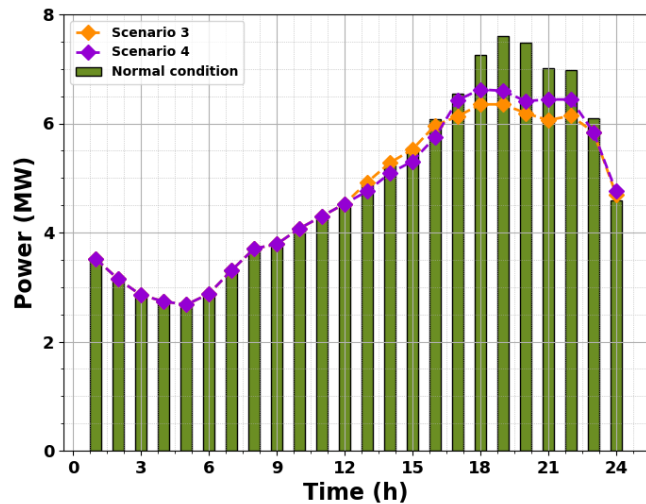


Figure 10. load changes in different scenarios in N-3 mode

5.3. IEEE 123 bus system

By moving the studied system to the IEEE 123 bus system, a modified single-phase network shown in Figure (11) is considered. This system consists of four common open lines 29-48, 39-66, 54-94, and 115-116. In this example, the penetration rate of scattered production sources reaches 26.04%. All faults are assumed to occur at 10:00 and repairs are scheduled for 22:00. Our detailed review includes two distinct yet typical scenarios:

- 1) Scenario 5: Simultaneous line outage is considered in lines 29-48, 13-18, and 105-108.
- 2) Scenario 6: Simultaneous line outage is considered in lines 18-21, 35-40, and 72--76.

Scenario 5 requires a total computation time of 1.258 s, while Scenario 6 is 0.841 s. Figure (11) and Figure (13) respectively show the optimal planning curves of microturbines and load reduction related to optimal topologies for both scenarios. Notably, scenario 6 shows a more pronounced load reduction due to lines 54-57 approaching its thermal limit after restructuring. Basically, the thermal limit of this line acts as the final determinant for load recovery during network restructuring. The lowest voltage recorded in scenario 5 and scenario 6 is 0.979 p.u. and 0.966 p.u. Is. It is important to emphasize that the bus voltages in the 123-bus system show a narrower range than their counterparts in the 69-bus system, due to the absence of lines characterized by significant impedances.

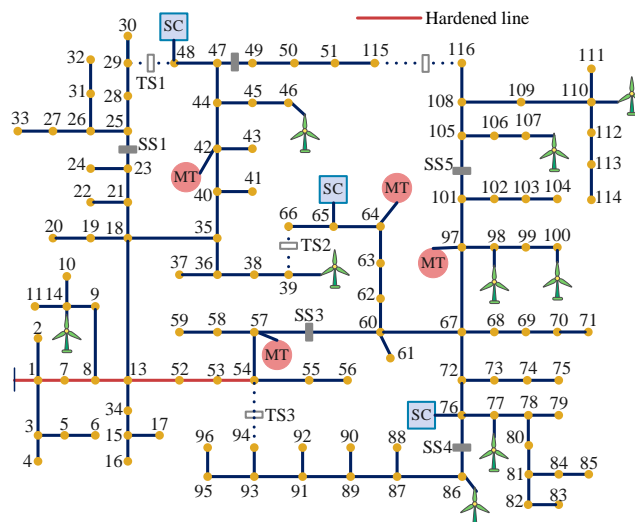


Figure 11. considered the IEEE 123 bus power system.

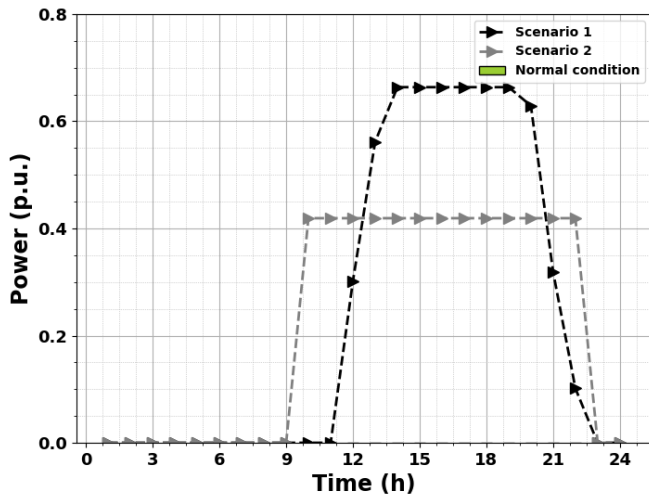


Figure 12. optimal micro turbine planning in different scenarios in IEEE 123 bus system

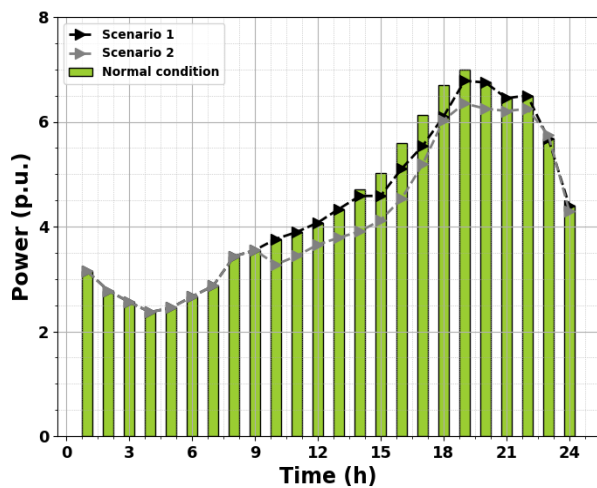


Figure 13. load changes in different scenarios in the IEEE 123 bus system

6. Conclusion

This study addresses critical challenges in enhancing the flexibility and reliability of distribution systems through a multi-faceted optimization approach. By integrating real-time network reconfiguration with the strategic deployment of distributed energy resources (DERs) and demand response programs (DRPs), significant improvements in system performance were achieved. The extensive case studies conducted on the IEEE 69-bus and IEEE 123-bus systems demonstrate the practical effectiveness of this approach. Key findings indicate that the proposed method effectively reduces outage durations, enhances fault tolerance, and improves voltage stability under various fault scenarios. The results from the IEEE 69-bus system, for instance, show that during scenarios involving two line faults, the optimization

framework reduced operational costs by up to 30% compared to traditional methods. Specifically, the cost reductions were \$4352 and \$5912 for scenarios 1 and 2, respectively. Additionally, in scenarios with three simultaneous line outages, the proposed approach achieved cost reductions of up to 22%, with operational costs of \$7329 in scenario 4 compared to \$8327 in scenario 3. These results highlight the framework's capability to provide cost-effective solutions and maintain system stability even under severe fault conditions. For the IEEE 123-bus system, the optimization framework demonstrated its robustness by maintaining voltage levels within acceptable limits, with the lowest recorded voltages being 0.979 p.u. and 0.966 p.u. in scenarios 5 and 6, respectively. This is notably better than the IEEE 69-bus system's performance, where voltage violations were more prevalent. The framework also managed to achieve a 26.04% penetration rate of scattered production sources, illustrating its effectiveness in integrating distributed generation. The contributions of this work are manifold. Firstly, it introduces a novel optimization framework that combines real-time network reconfiguration with DER and DRP strategies, offering a holistic approach to system management. Secondly, the study provides empirical evidence of the framework's effectiveness through detailed numerical simulations, demonstrating significant cost savings and improved system performance. Lastly, the research underscores the importance of adaptive and resilient grid operations, setting a new benchmark for future advancements in distribution system management.

Future research could further refine the optimization framework by exploring advanced computational techniques and incorporating more diverse fault scenarios. Additionally, examining the long-term impacts of such optimization strategies on system reliability and customer satisfaction could provide deeper insights into their overall benefits. The study lays a strong foundation for ongoing improvements in the field and offers valuable guidance for utilities and grid operators aiming to enhance the resilience and efficiency of their distribution networks.

Nomenclature

- N : Number of buses in the network
- L : Number of lines in the network
- B : Number of branches in the network
- G : Number of generators or distributed energy resources
- D : Number of demand points or loads
- i, j : Bus indices (where $i, j = 1, 2, \dots, N$)
- θ_i : Voltage angle at bus i
- V_i : Voltage magnitude at bus i
- x_{ij} : Reactance of the line connecting bus i and bus j
- R_{ij} : Resistance of the line connecting bus i and bus j
- S_{ij} : Complex power flow through the line connecting bus i and bus j
- P_i : Real power demand at bus i
- Q_i : Reactive power demand at bus i
- P_{gi} : Real power output from generator i
- Q_{gi} : Reactive power output from generator i
- ΔP_i : Change in real power at bus i due to reconfiguration or DRPs
- ΔQ_i : Change in reactive power at bus i due to reconfiguration or DRPs
- x : Decision variables in the optimization problem (e.g., switching states of network components)
- y : Auxiliary variables or parameters in the optimization problem
- DRP : Demand Response Program
- DG : Distributed Generation
- α_{dr} : Scaling factor for demand response
- β_{dg} : Capacity factor for distributed generation
- λ_{dr} : Price elasticity for demand response
- C_{ij} : Cost of reconfiguring the line between bus iii and bus jjj
- F_{ij} : Flow capacity of the line between bus iii and bus jjj
- R_{ijmax} : Maximum allowable current flow through the line between bus iii and bus jjj
- ATC : Available Transfer Capability
- CF : Congestion Factor
- η : Efficiency of the optimization algorithm
- δ : Deviation in power flow due to network changes
- F_i : Fault occurrence at bus i
- R_{fault} : Fault resistance in the network
- τ : Fault clearing time
- F : Objective function in optimization problems
- C : Constraint set in optimization problems
- A : Matrix of system coefficients in linear programming problems
- b : Vector of system constants in linear programming problems

Acknowledgments

This research was funded by the scientific research project of State Grid Hebei Energy Technology Service Co., Ltd. (23284503Z)

Reference

1. Tang, L., Han, Y., Zalhaf, A. S., Zhou, S., Yang, P., Wang, C., & Huang, T. (2024). Resilience enhancement of active distribution networks under extreme disaster scenarios: A comprehensive overview of fault location strategies. *Renewable and Sustainable Energy Reviews*, 189, 113898.
2. Ke, Q., Dong, D., Liu, T., Xiong, S., Jiang, W., Shi, X., & Lou, R. (2024). Review on development prospect of operation scheduling strategies for flexible interconnected distribution network in renewable energy-penetrated power system. *Journal of Computational Methods in Sciences and Engineering*, 24(2), 921-933. <https://doi.org/10.3233/JCM-247297>
3. Hosseini Kordkheili, A. Ghasemi-Marzbali, A. (2023). The Allocation of Optimal Capacity of Solar Sources to Achieve the Maximum Penetration Rate and Improve the Voltage Profile in Distribution Systems. *Iranian Electric Industry Journal of Quality and Productivity*, 12(2), 57-70.
4. Shi, Q., Li, F., Olama, M., Dong, J., Xue, Y., Starke, M., ... & Kuruganti, T. (2021). Network reconfiguration and distributed energy resource scheduling for improved distribution system resilience. *International Journal of Electrical Power & Energy Systems*, 124, 106355.
5. Jaramillo-Leon, B., Zambrano-Asanza, S., Franco, J. F., Soares, J., & Leite, J. B. (2024). Allocation and smart inverter setting of ground-mounted photovoltaic power plants for the maximization of hosting capacity in distribution networks. *Renewable Energy*, 223, 119968.
6. Candas, S., Baecker, B. R., Mohapatra, A., & Hamacher, T. (2023). Optimization-based framework for low-voltage grid reinforcement assessment under various levels of flexibility and coordination. *Applied Energy*, 343, 121147.
7. Shi, Q., Li, F., Olama, M., Dong, J., Xue, Y., Starke, M., ... & Kuruganti, T. (2021). Network reconfiguration and distributed energy resource scheduling for improved distribution system resilience. *International Journal of Electrical Power & Energy Systems*, 124, 106355.
8. Gantayet, A., & Dheer, D. K. (2022). A data-driven multi-objective optimization framework for optimal integration planning of solid-state transformer fed energy hub in a distribution network. *Engineering Science and Technology, an International Journal*, 36, 101278.
9. [Mahdavi, M., Alhelou, H. H., Hatziargyriou, N. D., & Jurado, F. (2021). Reconfiguration of electric power distribution systems: Comprehensive review and classification. *IEEE Access*, 9, 118502-118527. <https://doi.org/10.1109/ACCESS.2021.3107475>
10. Liu, F., Chen, C., Lin, C., Li, G., Xie, H., & Bie, Z. (2023). Utilizing aggregated distributed renewable energy sources with control coordination for resilient distribution system restoration. *IEEE Transactions on Sustainable Energy*, 14(2), 1043-1056. <https://doi.org/10.1109/TSTE.2023.3242357>
11. Igder, M. A., Liang, X., & Mitolo, M. (2022). Service restoration through microgrid formation in distribution networks: A review. *IEEE Access*, 10, 46618-46632. <https://doi.org/10.1109/ACCESS.2022.3171234>
12. Mahdavi, M., Alhelou, H. H., Bagheri, A., Djokic, S. Z., & Ramos, R. A. V. (2021). A comprehensive review of metaheuristic methods for the reconfiguration of electric power distribution systems and comparison with a novel approach based on efficient genetic algorithm. *IEEE Access*, 9, 122872-122906. <https://doi.org/10.1109/ACCESS.2021.3109247>
13. Ahrari, M., Shirini, K., Gharehveran, S. S., Ahsae, M. G., Haidari, S., & Anvari, P. (2024). A security-constrained robust optimization for energy management of active distribution networks with presence of energy storage and demand flexibility. *Journal of Energy Storage*, 84, 111024.
14. Javadi, E. A., Joorabian, M., & Barati, H. (2022). A sustainable framework for resilience enhancement of integrated energy systems in the presence of energy storage systems and fast-acting flexible loads. *Journal of Energy Storage*, 49, 104099.
15. Kahouli, O., Alsaiif, H., Bouteraa, Y., Ben Ali, N., & Chaabene, M. (2021). Power system reconfiguration in distribution network for improving reliability using genetic algorithm and particle swarm optimization. *Applied Sciences*, 11(7), 3092. <https://doi.org/10.3390/app11073092>

16. Caballero-Pena, J., Cadena-Zarate, C., Parrado-Duque, A., & Osma-Pinto, G. (2022). Distributed energy resources on distribution networks: A systematic review of modelling, simulation, metrics, and impacts. *International Journal of Electrical Power & Energy Systems*, 138, 107900.
17. Jangdoost, A., Keypour, R., & Golmohamadi, H. (2021). Optimization of distribution network reconfiguration by a novel RCA integrated with genetic algorithm. *Energy Systems*, 12(3), 801-833. <https://doi.org/10.1007/s12667-020-00398-5>
18. Zakaryaseraji, M., & Ghasemi-Marzbali, A. (2022). Evaluating congestion management of power system considering the demand response program and distributed generation. *International Transactions on Electrical Energy Systems*, 2022(1), 5818757.
19. Ortiz-Matos, L., Zea, L. B. G., & González-Sánchez, J. W. (2023). A methodology of sensor fault-tolerant control on a hierarchical control for hybrid microgrids. *IEEE Access*, 11, 58078-58098. <https://doi.org/10.1109/ACCESS.2023.3279821>
20. Home-Ortiz, J. M., Melgar-Dominguez, O. D., Javadi, M. S., Mantovani, J. R. S., & Catalao, J. P. (2022). Improvement of the distribution systems resilience via operational resources and demand response. *IEEE Transactions on Industry Applications*, 58(5), 5966-5976. <https://doi.org/10.1109/TIA.2022.3190241>
21. Aziz, T., Lin, Z., Waseem, M., & Liu, S. (2021). Review on optimization methodologies in transmission network reconfiguration of power systems for grid resilience. *International Transactions on Electrical Energy Systems*, 31(3), e12704.
22. Strezoski, L., Padullaparti, H., Ding, F., & Baggu, M. (2022). Integration of utility distributed energy resource management system and aggregators for evolving distribution system operators. *Journal of Modern Power Systems and Clean Energy*, 10(2), 277-285. <https://doi.org/10.35833/MPCE.2021.000667>
23. Ji, X., Yin, Z., Zhang, Y., & Xu, B. (2021). Real-time autonomous dynamic reconfiguration based on deep learning algorithm for distribution network. *Electric Power Systems Research*, 195, 107132.
24. Nawaz, A., Zhou, M., Wu, J., & Long, C. (2022). A comprehensive review on energy management, demand response, and coordination schemes utilization in multi-microgrids network. *Applied Energy*, 323, 119596.
25. [25] Schneider, K. P., Glass, J., Klauber, C., Ollis, B., Reno, M. J., Burck, M., ... & Yuan, G. (2022). A framework for coordinated self-assembly of networked microgrids using consensus algorithms. *IEEE Access*, 10, 3864-3878. <https://doi.org/10.1109/ACCESS.2021.3132253>
26. [26] Dunn, S., Wilkinson, S., Alderson, D., Fowler, H., & Galasso, C. (2018). Fragility curves for assessing the resilience of electricity networks constructed from an extensive fault database. *Natural Hazards Review*, 19(1), 04017019. [https://doi.org/10.1061/\(ASCE\)NH.1527-6996.0000267](https://doi.org/10.1061/(ASCE)NH.1527-6996.0000267)
27. Yuan, H., Li, F., Wei, Y., & Zhu, J. (2016). Novel linearized power flow and linearized OPF models for active distribution networks with application in distribution LMP. *IEEE Transactions on Smart Grid*, 9(1), 438-448. <https://doi.org/10.1109/TSG.2016.2594814>
28. Ding, T., Lin, Y., Bie, Z., & Chen, C. (2017). A resilient microgrid formation strategy for load restoration considering master-slave distributed generators and topology reconfiguration. *Applied energy*, 199, 205-216. <https://doi.org/10.1016/j.apenergy.2017.05.012>
29. James, J. Q., & Li, V. O. (2015). A social spider algorithm for global optimization. *Applied soft computing*, 30, 614-627. <https://doi.org/10.1016/j.asoc.2015.02.014>
30. Cikan, M., & Cikan, N. N. (2023). Optimum allocation of multiple type and number of DG units based on IEEE 123-bus unbalanced multi-phase power distribution system. *International Journal of Electrical Power & Energy Systems*, 144, 108564.